




Cite this: *RSC Adv.*, 2020, 10, 12053

Cu(II) vitamin C tunes photocatalytic activity of TiO₂ nanoparticles for visible light-driven aerobic oxidation of benzylic alcohols†

Narges Pourmorteza, Maasoumeh Jafarpour, * Fahimeh Feizpour and Abdolreza Rezaeifard *

The incorporation of Cu(OAc)₂ into ascorbic acid coated TiO₂ nanoparticles easily provided a new heterogeneous visible-light active titania-based photocatalyst (TiO₂-AA-Cu(II)) which was characterized by different techniques such as FT-IR, XPS, ICP-AES, TGA and TEM. A red-shift of the band-edge and a reduction of the band-gap (2.8 eV vs. 3.08 for TiO₂) were demonstrated by UV-DRS and Tauc plots. The combination of the as-prepared TiO₂-AA-Cu(II) nanoparticles with TEMPO and molecular oxygen (air) afforded an active catalytic system for the selective oxidation of diverse set of benzylic alcohols under solvent-free conditions. A photoassisted pathway was confirmed for oxidation reactions evidenced by good correlation between apparent quantum yield (AQY) and diffuse reflectance spectra (DRS) of the as-prepared nanohybrid. The spectral data and recycling experiments demonstrated the structural stability of the title copper photocatalyst during oxidation reactions.

Received 3rd January 2020

Accepted 15th March 2020

DOI: 10.1039/d0ra00075b

rsc.li/rsc-advances

1 Introduction

Transition metal ions are playing an important role in biological processes in the human body.^{1,2} They are found either at the active sites or as structural components of a good number of enzymes.^{3,4} Thus, study of the coordination chemistry of biologically important metal ions with bio-relevant ligands has been always an active research subject in bio-inorganic chemistry. In this line of research, metal containing vitamins are increasingly becoming important particularly in drug design and nutrition, with the hope of improving and enriching the quality of existing vitamins, thereby serving as a better substitute as chemotherapeutic agents.^{5–7} In the search for novel metal complexes, that combine high activity with low toxicity, the study of metal complexes has continued to attract attention of some coordination chemists.^{8–10} This has also provided useful outlets for basic research in coordination chemistry. Among metal containing vitamins, the Cu(II) vitamin C complex attracted the most attention, because both Cu²⁺ and vitamin C are essential for the biosynthesis of the pigment melanin and are preferentially absorbed by the malignant melanoma tissues. There are also invaluable

reports regarding the combination of Cu²⁺ and ascorbate (vitamin C) halt tumor growth in mice.^{11,12}

As a part of our ongoing project, developing new visible light driven photocatalytic systems by surface modification of TiO₂ nanoparticles by vitamins-metal complexes,^{13–15} in the present study, a novel heterogeneous nanostructured bio-photocatalyst is prepared by incorporation of simple and easily available Cu(OAc)₂ compound into ascorbic acid-coated TiO₂ nanoparticles under ultrasonic agitation. Copper-vitamin C complex supported on TiO₂ nanoparticles is explored as an active photocatalyst for the selective oxidation of benzylic alcohols *via* ideal green process, *i.e.* using molecular oxygen in air as oxidant and be free of any solvent under visible light irradiation (Scheme 1). Spectral data, leaching experiment and recycling test proved the stability of the as-prepared nanohybrid making it competent catalyst for practical goals.

2. Experimental

Note: general remarks and step by step preparation of TiO₂-AA-Cu(II) nanohybrid catalyst are given in ESI.†

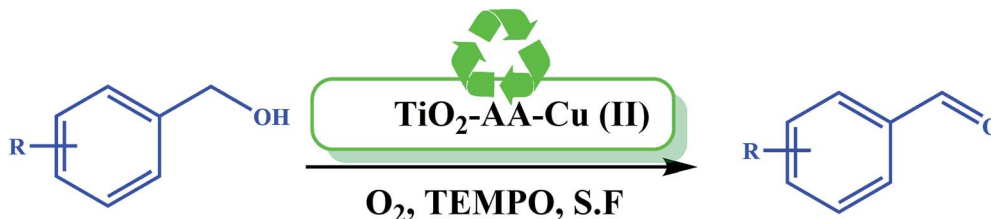
2.1. General procedure for aerobic oxidation of benzylic alcohols catalyzed by TiO₂-AA-Cu(II) nanohybrid

To a mixture of benzyl alcohols (0.125 mmol) and TiO₂-AA-Cu(II) nanohybrid (3 mg) was added TEMPO (0.0192 mmol) and the reaction mixture was stirred at 70 °C under air, visible light using a full spectrum CFL bulb (40 W) and solvent free conditions for the required time. The reaction progress and the yields

Catalysis Research Laboratory, Department of Chemistry, Faculty of Science, University of Birjand, Birjand, 97179-414, Iran. E-mail: mjafarpour@birjand.ac.ir; Jafarpouryas@gmail.com; rrezaeifard@birjand.ac.ir; Tel: +98 5632202515; +98 5632202516

† Electronic supplementary information (ESI) available. See DOI: 10.1039/d0ra00075b





Scheme 1 Aerobic oxidation of benzyl alcohols in the presence of $\text{TiO}_2\text{-AA-Cu(II)}$ nanohybrid.

of the products were monitored by GC. The isolated products were obtained by plate chromatography eluted with *n*-hexane/ethylacetate (10 : 3).

3. Result and discussion

3.1. Synthesis and characterization of $\text{TiO}_2\text{-AA-Cu(II)}$ nanohybrid

First, TiO_2 and $\text{TiO}_2\text{-AA}$ nanoparticles were synthesized and purified according to our previous report¹⁶ (for experimental details, see the ESI†). For fabrication of $\text{TiO}_2\text{-AA-Cu(II)}$ nanohybrid, 0.2 g of $\text{TiO}_2\text{-AA}$ is dispersed in 5 mL deionized (DI) water through sonication for 5 min. Then, 1.0 mmol Cu(OAc)_2 dissolved in ethanol is dropped into the suspension under ultrasonic agitation at room temperature for 20 min. The as-obtained mixture is refluxed for 12 h (Scheme S1†). Afterwards, the obtained product is centrifuged, washed with ethanol and dried at 100 °C for 12 h under vacuum. The Cu content of as-prepared catalyst was 1.23% based on ICP-AES analysis.

TEM images of nanohybrid exhibited a spherical morphology with an average size of 10–15 nm (Fig. S1†).

Comparative FT-IR spectra of TiO_2 , $\text{TiO}_2\text{-AA}$ and $\text{TiO}_2\text{-AA-Cu(II)}$ nanohybrid depicted in Fig. 1, confirms the complexation

of Cu(II) with AA coated TiO_2 . As depicted in Fig. 1, all of the samples show a broad peak at around 3000 cm^{-1} corresponding to the hydroxyl groups. Broad peak at 1625 cm^{-1} corresponds to the surface adsorbed water. The bands in the region of $500\text{--}750\text{ cm}^{-1}$ are attributed to the stretching vibrations of Ti–O groups.¹⁷ The coating of AA on TiO_2 (Fig. 1b) is substantiated by C–O stretching vibration of Ti–O–C appeared in the range of 927 and 984 cm^{-1} .¹⁸ The strong peaks at about 1411 and 1560 cm^{-1} are attributed to the acetate group. The appearance of a band at 563 cm^{-1} in Fig. 1c is rationalized to the stretching vibration of Cu–O bond.¹⁹

The survey XPS spectrum of $\text{TiO}_2\text{-AA-Cu(II)}$ nanohybrid reveals the presence of Ti 2p, Cu 2p, O 1s and C elements (Fig. 2). Two broad peaks at 458 and 464 eV are attributed to the Ti 2p_{3/2} and Ti 2p_{1/2}, respectively.²⁰ The peak at 531 eV is assigned to the O 1s.²¹ Also, the signals at 935.32 and 955.28 eV correspond to 2p_{3/2} and 2p_{1/2} of Cu(II), respectively.^{22–24}

TGA curve of catalyst (Fig. S2†) demonstrates its thermostability up to 200 °C and the organic parts decomposed completely at 678 °C.

Tauc plot, $(\alpha h\nu)^2$ vs. $(h\nu)$, was used to determine the optical bandgap. As shown in Fig. 3, the band gap of TiO_2 (3.08 eV) reduced gradually during modification with AA ($\text{TiO}_2\text{-AA}$, 3.0 eV) and complexation with Cu(II) (Cu-AA-Cu(II) , 2.8 eV) making it a visible-light sensitive photocatalyst.

3.2. Photo-induced aerobic oxidation of benzylic alcohols

Oxidation of 4-chlorobenzyl alcohol (0.125 mmol) in the presence of $\text{TiO}_2\text{-AA-Cu(II)}$ /TEMPO photocatalytic system was chosen as a model reaction. A series of experiments was conducted to optimize the effect of solvent, amount of catalyst and TEMPO, temperature, and nature of oxidants (Fig. S3 and S4†).

According to optimization experiments the reaction proceeds more effective in the absence of any solvent (Fig. S3a†). A temperature variation study showed that the conversion steadily increases from 50 to 90% as the temperature increases from 25 to 70 °C with maintaining the selectivity (Fig. S3b†). A survey of the results shown in Fig. S3c† revealed that a catalyst loading of 3 mg (0.4 mol% based on Cu) leads to the desired yield of product. Also, we found that TEMPO is essential to trigger the reaction and access to the highest catalytic performance (Fig. S3d†). When air was replaced by pure O_2 as well as commercially available oxidants, less activity and selectivity were observed (Fig. S3e†). The parent materials such as TiO_2 , $\text{TiO}_2\text{-AA}$, AA, Cu(OAc)_2 and also ZnO were inferior under optimized conditions (Fig. S4†). Thus, title catalytic aerobic

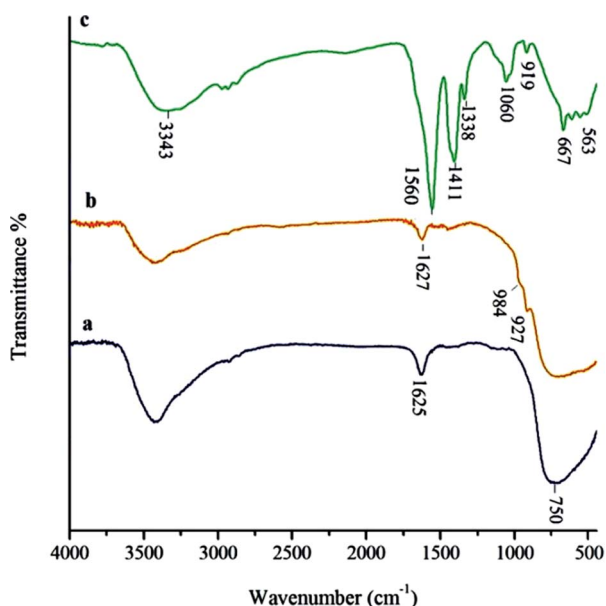


Fig. 1 FT-IR spectra of (a) nanostructure TiO_2 (b) $\text{TiO}_2\text{-AA}$ (c) $\text{TiO}_2\text{-AA-Cu(II)}$ nanohybrid.



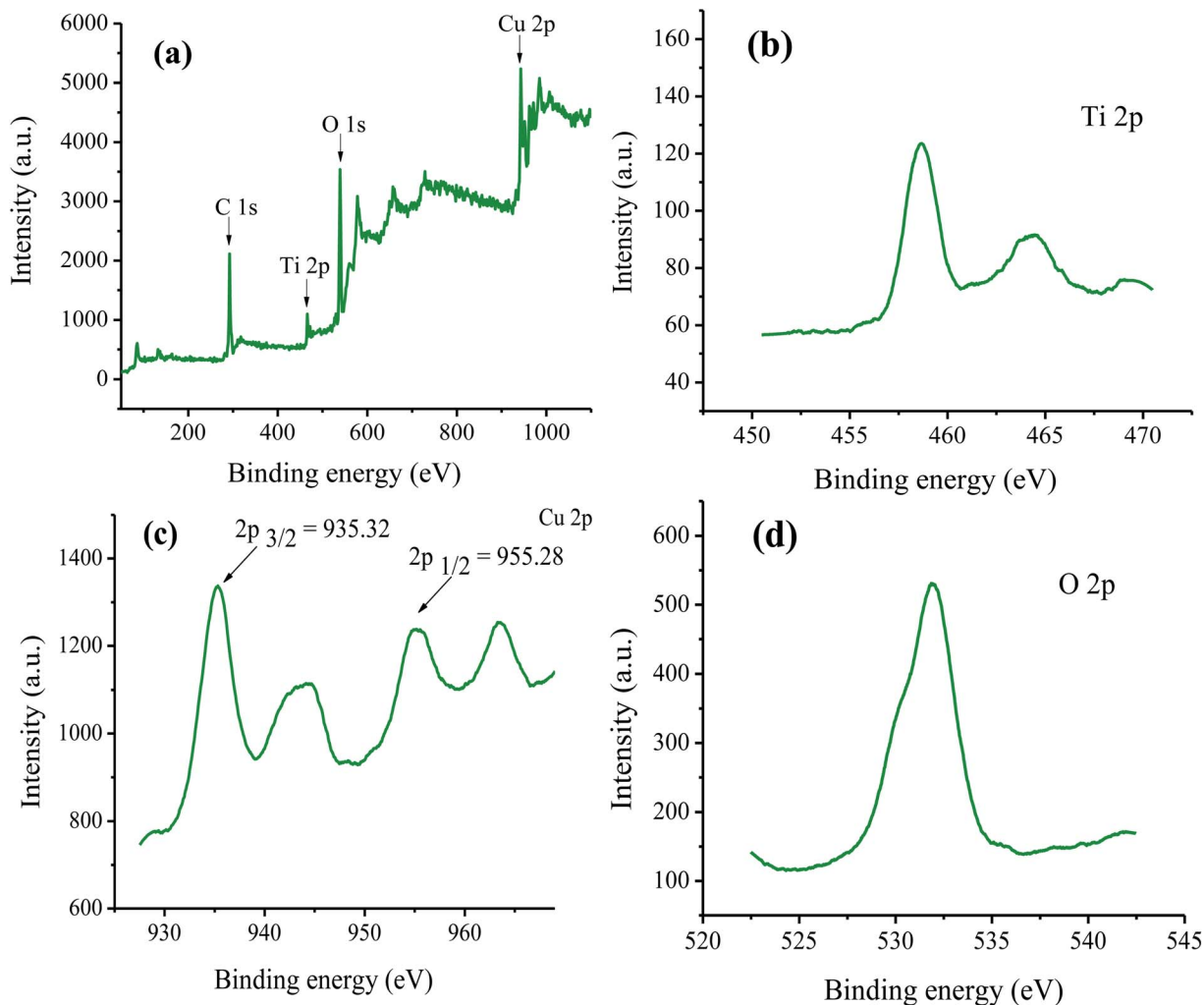


Fig. 2 XPS spectra of $\text{TiO}_2\text{-AA-Cu(II)}$ nanohybrid (a) wide scan, (b) Ti 2p, (c) Cu 2p, and (d) O 1s.

procedure exhibits the highest efficiency under visible light irradiation, using a benzyl alcohol : TEMPO molar ratio of 6.5 (0.125 : 0.0192) and 3 mg (0.4 mol% based on Cu) catalyst under solvent free conditions at 70 °C.

Next, we subjected various benzylic alcohols to the reaction conditions to assess the scope of the method. Our data summarized in Table 1 demonstrated the high efficiency of the title photocatalytic system for the visible light-induced aerobic oxidation of structurally and electronically different benzylic alcohols.

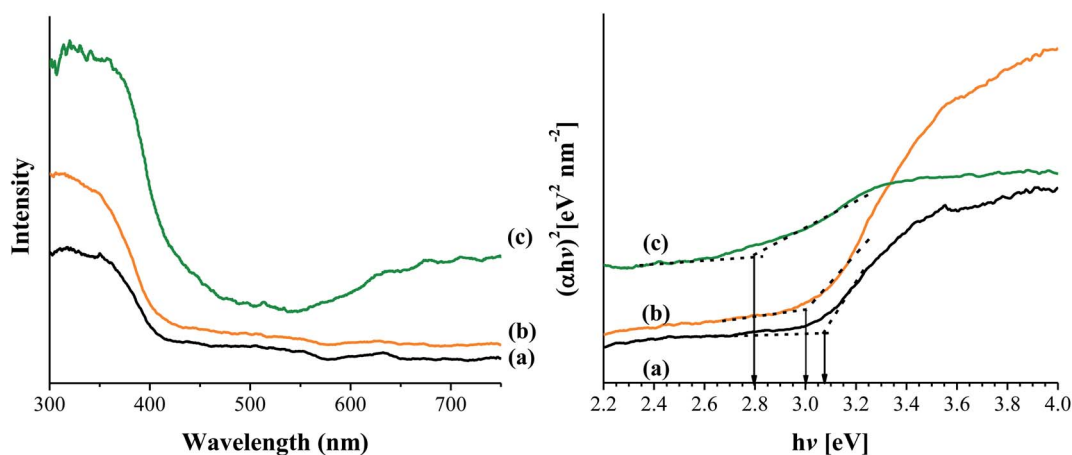


Fig. 3 UV-Vis spectra and DRS of (a) bare TiO_2 NPs, (b) $\text{TiO}_2\text{-AA}$ and (c) $\text{TiO}_2\text{-AA-Cu(II)}$ nanohybrid.

Table 1 Oxidation of benzylic alcohols in the presence of TiO_2 -AA-Cu(III)^a

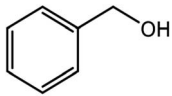
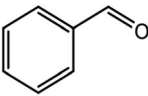
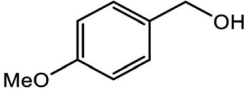
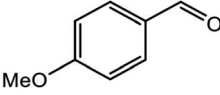
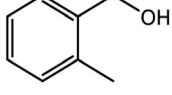
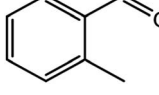
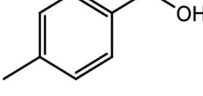
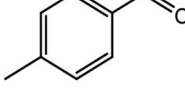
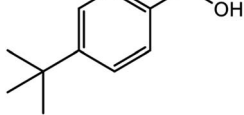
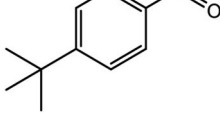
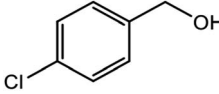
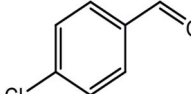
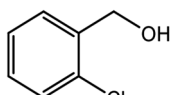
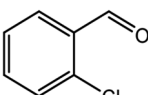
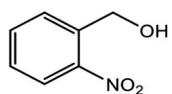
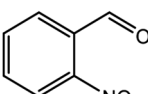
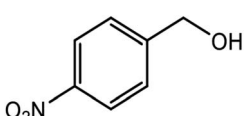
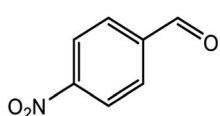
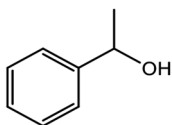
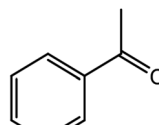
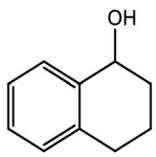
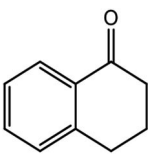
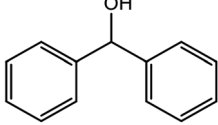
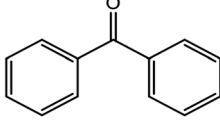
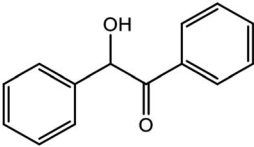
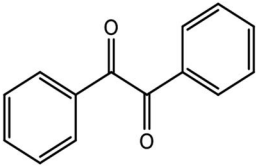
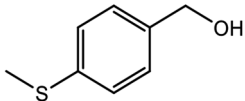
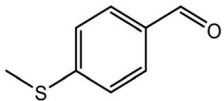
| Entry | Alcohol | Product ^b | Isolated yield ^c (%) |
|-------|---|--|---------------------------------|
| 1 |  |  | 96 |
| 2 |  |  | 96 |
| 3 |  |  | 94 |
| 4 |  |  | 96 |
| 5 |  |  | 89 |
| 6 |  |  | 95 |
| 7 |  |  | 94 |
| 8 |  |  | 60 (3 h) |
| 9 |  |  | 68 (3 h) |
| 10 |  |  | 98 |
| 11 |  |  | 68 (5 h) |
| 12 |  |  | 78 (5 h) |



Table 1 (Contd.)

| Entry | Alcohol | Product ^b | Isolated yield ^c (%) |
|-----------------|---|--|---------------------------------|
| 13 |  |  | 85 |
| 14 ^d |  |  | 85 (6 h) |

^a Reaction condition: 0.125 mmol alcohol, TEMPO (0.0192 mmol), cat. (0.003 g) and the reactions were run under solvent free conditions at 70 °C for 2 h under air and visible light (CFL, 40 W). ^b The products were identified by comparison with authentic sample retention times of GC analysis and NMR spectra. ^c The selectivity of products were >99% based on GC analysis. ^d 15% of (4-methanesulfinyl-phenyl)-methanol was obtained.

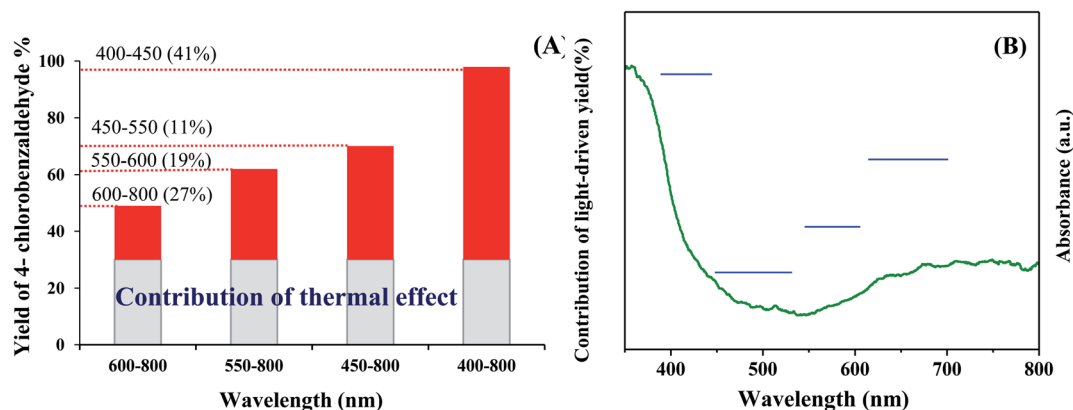


Fig. 4 Dependence of 4-chlorobenzaldehyde yield on the irradiation wavelength (A), and the action spectrum of the photocatalytic reaction, in which the light driven conversion is plotted against the irradiation wavelength (B).

However, the oxidation performance affected by electronic properties of substrates. Electron-withdrawing groups on the phenyl rings of alcohols retarded the reaction (Table 1, entries 8 and 9). Both primary and secondary benzylic alcohols delivered the corresponding carbonyl compounds in good to excellent yields. It should be mentioned that no trace of ester or benzoic acid was observed resulting from over oxidation of secondary and primary alcohols, respectively. To demonstrate the chemoselectivity of the method, 4-methylsulfonyl benzyl alcohol carrying oxidative sensitive sulfur atom was subjected to the oxidation procedure. The related carbonyl compound was formed as major product (85%) accompanied with 15% of the pertinent sulfoxide (4-methanesulfinyl-phenyl)-methanol resulting from sulfide group oxidation (Table 1, entry 14). It should be noted that the photocatalytic system was unable to oxidize the aliphatic alcohols and heterocyclic alcohols under different conditions.

3.3. Photocatalytic activity

The photocatalytic activity of TiO₂-AA-Cu(II) nanohybrid was investigated by the oxidation of 4-chlorobenzyl alcohol under

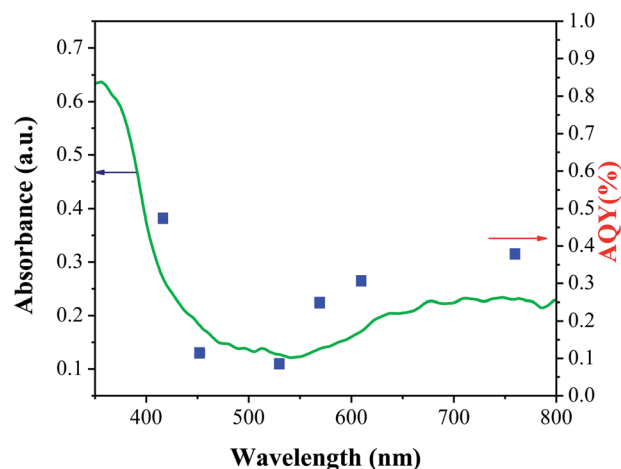


Fig. 5 Photocatalytic action spectrum for synthesis of 4-chlorobenzaldehyde using TiO₂-AA-Cu(II) photocatalyst.



Table 2 Comparison of oxidative activity of TiO₂-AA-Cu(II) nanohybrid with other Cu based catalysts in the oxidation of benzyl alcohol

| Entry | Catalyst | Catalyst (mol%) | Conditions | Time (h) | Yield (%) | Ref. |
|-------|--|--------------------|---|----------|-----------|-----------|
| 1 | TiO ₂ -AA-Cu(II) | 0.003 g (0.4 mol%) | 70 °C/s.f/TEMPO/vis. light/air | 2 | 96 | This work |
| 2 | SBA@AP ^a -L _{Pro} ^b -CuOAc | 1 | 50 °C/toluene/TEMPO/Cs ₂ CO ₃ /O ₂ | 9 | 90 | 26 |
| 3 | Salophen-copper(II) | 2 | rt/MeCN/TBHP/NaOH/air | 24 | 97 | 27 |
| 4 | CuCl | 5 | rt/DMAP ^c /TEMPO/H ₂ O/air | 10 | 94 | 28 |
| 5 | PS ^d -PEG-TD ₂ ^e Cu(OAc) ₂ | 20 | 80 °C/heptane/TEMPO/air | 24 | 80 | 29 |
| 6 | [Cu(L ^{allyl}) ₂] ^f | 0.025 mmol | 25 °C/toluene/TEMPO/air | 18 | 97 | 30 |
| 7 | CuBr/UiO-66-NH-PC ^g | 5 | rt/CH ₃ CN/TEMPO/NMI ^h /air | 9 | 86 | 31 |
| 8 | [MCM-41-bpy-CuI] | 5 | 50 °C/EtOH/TEMPO/NH ₃ /air | 26 | 92 | 32 |
| 9 | CuO-rectorite | 31 mg | 50 °C/H ₂ O/K ₂ CO ₃ /TEMPO/O ₂ | 24 | 77.8 | 33 |
| 10 | (NH ₄) ₄ [CuMo ₆ O ₁₈ (OH) ₆] | 1 | 60 °C/MeCN : H ₂ O/NaCl/O ₂ | 20 | 87 | 34 |
| 11 | Cu-Mn oxide/C | 10 wt% | 80 °C/CH ₂ Cl ₂ /TEMPO/O ₂ | 2.5 | 96.9 | 35 |
| 12 | CuFe ₂ O ₄ | 10 | 100 °C/H ₂ O/TEMPO/O ₂ | 24 | 79 | 36 |
| 13 | CuBr | 5 | rt/CH ₃ OH/L-proline/Na ₂ CO ₃ /TEMPO/air | 6 | 92 | 37 |

^a (3-Aminopropyl) triethoxysilane. ^b (S)-1-(3,5-Dichloro-2-hydroxybenzyl) pyrrolidine-2-carboxylic acid. ^c 4-Dimethylaminopyridine. ^d Polystyrene.

^e Triazine-based polyethyleneamine dendrimer. ^f N-Allyl-o-hydroxyacetophenoniminato. ^g Picolinoyl chloride. ^h N-Methylimidazole.

air as oxidant. The visible-light source for the photocatalytic reaction was a 40 W CFL bulb (400 to 800 nm) equipped with different cut-off filters. A reaction subjected on the full spectrum irradiation (without any cut-off filters) gives 98% 4-chlorobenzaldehyde (GC yield). Nevertheless, the product yield decreased to 70, 62, and 49%, by employing 450–800, 550–800, and 600–800 nm filters, respectively. The contributions of the photoassisted pathway by deducting the thermal contribution (product formed at dark; 30%) are 41, 11, 19 and 27% for 400–450, 450–550, 550–600 and 600–800 nm, respectively (Fig. 4). These results are consistent with the UV-visible absorption spectrum and band gap value of 2.8 eV of TiO₂-AA-Cu(II) nanohybrid and demonstrate the highest visible-light photocatalytic performance of catalyst at 400–450 nm (Fig. 4).

More evidence for the photocatalytic activity of as-prepared catalyst was obtained by apparent quantum yield for 4-chlorobenzaldehyde formation (AQY) calculated with the following equation: [AQY (%) = (%) $Y_{vis} - Y_{dark} \times 2 / (\text{photon number entered into the reaction vessel}) \times 100$].²⁵ Fig. 5 clearly shows a good correlation between AQY and diffuse reflectance spectrum (DRS) of the TiO₂-AA-Cu(II) nanohybrid confirming once again a photoassisted pathway for title oxidation reactions.

3.4. Catalyst recovery and reuse

The stability and reusability of TiO₂-AA-Cu(II) nanohybrid were assessed during 4 runs (Fig. S5†). At the end of each run, 2 mL ethanol as a green solvent was added, followed by centrifugation to isolate the residual catalyst. The catalyst was dried under vacuum and reused for next runs. The negligible loss of activity was observed during 4 runs revealed the structural stability of the catalyst. More evidences for this important issue were obtained by monitoring the FT-IR spectra of catalyst during 4 cycles (Fig. S6†) as well as lack of copper in filtrate based on leaching hot filtration test combined with ICP-AES analysis.

Table 2 lists some aerobic methods based on Cu catalysts for oxidation of benzyl alcohol in comparison with the present catalytic system. The obvious advantages of our

photochemical method including a visible light-induced catalyst with low dosage and high recyclability, desired reaction time, high product yield and excellent selectivity and particularly environmentally benign conditions used in this work (solvent-free condition under air and visible light irradiation) qualify all requirements of an efficient catalytic system for applied goals.

4 Conclusion

In conclusion, an efficient and clean aerobic method for visible light-driven photooxidation of benzylic alcohols over TiO₂-AA-Cu(II) nanohybrid in combination with TEMPO under solvent-free condition was developed. The catalyst showed desired recyclability and no copper leaching was observed during reaction, which demonstrates its potential for industrial application. Good correlation between apparent quantum yield (AQY) and diffuse reflectance spectrum (DRS) of the as-prepared nanohybrid confirmed a photoassisted pathway for the title oxidation reactions. The use of air as oxidant and visible light as a safe light source under solvent-free condition in the presence of a reusable and selective bio-relevant oxidation catalyst offer an ideal green protocol, making it more appropriate for applied goals.

Conflicts of interest

The authors declare no conflict of interest.

Acknowledgements

Support for this work by Research Council of University of Birjand and "Iran national Science Foundation" (Grant No. 96013225) is highly appreciated.

References

- 1 W. W. Zhao, J. J. Xu and H. Y. Chen, *Analyst*, 2016, **141**, 4262–4271.



- 2 S. Kapoor, D. Brazete, I. C. Pereira, G. Bhatia, M. Kaur, L. F. Santos and J. M. Ferreira, *J. Non-Cryst. Solids*, 2019, **506**, 98–108.
- 3 C. A. Denard, H. Huang, M. J. Bartlett, L. Lu, Y. Tan, H. Zhao and J. F. Hartwig, *Angew. Chem., Int. Ed.*, 2014, **53**, 465–469.
- 4 J. M. Palomo and M. Filice, *Biotechnol. Adv.*, 2015, **33**, 605–613.
- 5 D. A. Kose, B. Zumreoglu-Karan, C. Unaleroglu, O. Sahin and O. Buyukgungor, *J. Coord. Chem.*, 2006, **59**, 2125–2133.
- 6 A. E. Fazary, Y.-H. Ju, A. Q. Rajhi, A. S. Alshihri, M. Y. Alfaifi, M. A. Alshehri, K. A. Saleh, S. E. I. Elbehairi, K. F. Fawy and H. S. M. Abd-Rabboh, *Open Chem.*, 2016, **14**, 287–298.
- 7 P. Brandão and S. Guieu, in *Mol. Nutr.*, Elsevier, 2020, pp. 33–49.
- 8 A. Pettenuzzo, R. Pigot and L. Ronconi, *Eur. J. Inorg. Chem.*, 2017, **2017**, 1625–1638.
- 9 B. Annaraj and M. A. Neelakantan, *Eur. J. Med. Chem.*, 2015, **102**, 1–8.
- 10 A. K. Renfrew, *Metalomics*, 2014, **6**, 1324–1335.
- 11 B. Zümreoglu-Karan, *Coord. Chem. Rev.*, 2006, **250**, 2295–2307.
- 12 Y.-D. Park, Y.-J. Lyou, H.-S. Hahn, M.-J. Hahn and J.-M. Yang, *J. Biomol. Struct. Dyn.*, 2006, **24**, 131–138.
- 13 F. Feizpour, M. Jafarpour and A. Rezaeifard, *Catal. Lett.*, 2018, **148**, 30–40.
- 14 F. Feizpour, M. Jafarpour and A. Rezaeifard, *Catal. Lett.*, 2019, **149**, 1595–1610.
- 15 E. Rezapour, M. Jafarpour and A. Rezaeifard, *Catal. Lett.*, 2018, **148**, 3165–3177.
- 16 M. Jafarpour, F. Feizpour and A. Rezaeifard, *RSC Adv.*, 2016, **6**, 54649–54660.
- 17 G. Li, B. Wang, W. Q. Xu, Y. Han and Q. Sun, *Dyes Pigm.*, 2018, **155**, 265–275.
- 18 Y. Ou, J.-D. Lin, H.-M. Zou and D.-W. Liao, *J. Mol. Catal. A: Chem.*, 2005, **241**, 59–64.
- 19 Z. Ansari, A. Saha, S. S. Singha and K. Sen, *J. Photochem. Photobiol., A*, 2018, **367**, 200–211.
- 20 S. Mathew, P. Ganguly, S. Rhatigan, V. Kumaravel, C. Byrne, S. Hinder, J. Bartlett, M. Nolan and S. Pillai, *Appl. Sci.*, 2018, **8**, 2067.
- 21 Q. Hu, J. Huang, G. Li, Y. Jiang, H. Lan, W. Guo and Y. Cao, *Appl. Surf. Sci.*, 2016, **382**, 170–177.
- 22 T. Zheng, T. Wang, R. Ma, W. Liu, F. Cui and W. Sun, *Sci. Total Environ.*, 2019, **650**, 1412–1418.
- 23 J. Kim, T. Kang, H. Kim, H. J. Shin and S.-G. Oh, *J. Ind. Eng. Chem.*, 2019, **77**, 273–279.
- 24 S. E. Allen, R. R. Walvoord, R. Padilla-Salinas and M. C. Kozlowski, *Chem. Rev.*, 2013, **113**, 6234–6458.
- 25 Y. Sugano, Y. Shiraishi, D. Tsukamoto, S. Ichikawa, S. Tanaka and T. Hirai, *Angew. Chem., Int. Ed.*, 2013, **52**, 5295–5299.
- 26 I. Saberikia, E. Safaei, B. Karimi and Y.-I. Lee, *ChemistrySelect*, 2017, **2**, 11164–11171.
- 27 T. Chen and C. Cai, *Synth. Commun.*, 2015, **45**, 1334–1341.
- 28 G. Zhang, C. Yang, E. Liu, L. Li, J. A. Golen and A. L. Rheingold, *RSC Adv.*, 2014, **4**, 61907–61911.
- 29 S. Pan, S. Yan, T. Osako and Y. Uozumi, *Synlett*, 2018, **29**, 1152–1156.
- 30 M. del Mar Conejo, P. Ávila, E. Álvarez and A. Galindo, *Inorg. Chim. Acta*, 2017, **455**, 638–644.
- 31 X. Du, Y. Luan, F. Yang, D. Ramella and X. Shu, *New J. Chem.*, 2017, **41**, 4400–4405.
- 32 H. Zhao, Q. Chen, L. Wei, Y. Jiang and M. Cai, *Tetrahedron*, 2015, **71**, 8725–8731.
- 33 W. Liu, J. Yang and J. Cai, *Res. Chem. Intermed.*, 2019, **45**, 549–561.
- 34 Y. Wei, Z. Wei, S. Ru, Q. Zhao, H. Yu and G. Zhang, *Green Chem.*, 2019, **21**, 4069–4075.
- 35 G. Yang, W. Zhu, P. Zhang, H. Xue, W. Wang, J. Tian and M. Song, *Adv. Synth. Catal.*, 2008, **350**, 542–546.
- 36 X. Zhu, D. Yang, W. Wei, M. Jiang, L. Li, X. Zhu, J. You and H. Wang, *RSC Adv.*, 2014, **4**, 64930–64935.
- 37 G. Zhang, X. Han, Y. Luan, Y. Wang, X. Wen and C. Ding, *Chem. Commun.*, 2013, **49**, 7908–7910.

